THE ANNALS OF "DUNAREA DE JOS" UNIVERSITY OF GALATI
FASCICLE IX. METALLURGY AND MATERIALS SCIENCE
Nº. 2 - 2015, ISSN 1453 – 083X

EFFECTIVE ELECTROMECHANICAL COUPLING FOR THE PARTIALLY ELECTRODED CERAMIC RESONATORS OF DIFFERENT GEOMETRIES

Jiří Erhart* and Tutu Sebastian
Department of Physics and Piezoelectricity Research Laboratory, Technical University of Liberec, Studentská 2, 461 17 Liberec 1, Czech Republic
*corresponding author
e-mail: jiri.erhart@tul.cz

ABSTRACT

Effective electromechanical coupling factor (ECF) was studied on bar, disc and ring ceramic resonators partially covered by electrodes. ECFs were calculated theoretically and verified experimentally. Bar resonators (k_{31}-mode) show maximum value of ECF k_{eff} = 0.26 at the electrode aspect ratio equal to 0.75 with calculated values fitting the experimental data for all aspect ratios. Calculations for bar resonators with embedded electrodes (k_{33}-mode) show similar behavior like for k_{31}-mode, but at higher ECFs. Maximum value of ECF for such a mode reaches k_{eff} = 0.67 for the electrode aspect ratio of 0.75. Partially electroded disc resonators (k_p-mode) are well described analytically by one-dimensional model only for the electrode aspect ratios up to 0.5. Maximum value k_{eff} = 0.58 for disc resonators was measured at the electrode aspect ratio equal to 0.80. Partially electroded ring resonators (k_p-mode) show the same trend as discs without saturation of ECF values. Maximum ECF k_{eff} = 0.34 was measured for ring resonators with full electrode. The presented analytical formulae may serve as a guide for the optimum electrode pattern design for the partially electroded resonators.

KEYWORDS: piezoelectric ceramics, PZT, resonator, vibration modes, electromechanical coupling factor

1. Introduction

Electromechanical coupling factor (ECF) describes the energy transfer between its mechanical and electrical form. Static electromechanical coupling might be different from the dynamic coupling factor specific for certain vibration modes [1]. ECF links together "free" and "clamped" material properties for different resonators shapes. ECFs for different vibration modes are also cross-linked by various relations [2].

ECFs are practically measured using the analysis of impedance spectrum in terms of resonance (f_r) and antiresonance (f_a) frequencies [1, 3] with an effective dynamic coupling factor

$$k_{eff}^2 = \frac{f_a^2 - f_r^2}{f_a^2} \qquad (1)$$

This formula is universal for any vibration mode of resonators, but there are also specific formulae for the different vibration modes of resonators (e.g. k_{31}, k_{33}, k_p, k_t, k_{15} modes) in the shape of bar, thin disc or plate [3]. Resonators for ECF measurement are designed as fully electroded piezoelectric ceramic bodies. Such resonators are not necessarily optimized with respect to ECF value.

It is basically anticipated that the piezoelectric resonator with full electrode has its maximum electromechanical coupling. However, sometimes it is not possible to deposit the full electrode on the piezoelectric resonator faces because of the mechanical clamping or electrical insulation of the resonator. Small facet at the piezoelectric ceramic ring or disc edges is one of the examples of such electrode deposition deficiency. There is also the possibility of ECF enhancement by the electrode pattern optimization.

The experimental visualization of modal shapes was published for fully electroded ceramic disc

resonators for the radial and flexural vibration modes and verified by laser holography [4]. A similar visualization was also performed by the same technique on the partially electroded discs in two geometries [5] – disc with central circular electrode or with annular electrode arrangement. The optimum electromechanical coupling k = 0.605 for the disc planar mode was theoretically calculated for the electrode size ratio r_0 = 0.83a for PIC-151 PZT ceramics (r_0, a are the radii of electrode and disc).

Theoretical calculations on partially electroded disc ceramic resonators were published by Ivina [6]. A ceramic disc was partially electroded inside the central circular area or at the outer annular electrode. The optimum ECF k = 0.51 was calculated for the central circular electrode size ratio r_0 = 0.9a for TsTBS-3 PZT type. The enhancement of ECF for the partially electroded disc (k = 0.51) with respect to the fully electroded one (k = 0.50) was calculated. The ceramic resonator operates more efficiently with optimum electrode size than with the full electrode.

Other theoretical calculations on the partially covered ceramic resonators were published by Rogacheva [7]. She calculated ECFs for several electrode geometries – disc plate with central circular or ring electrode and cylindrical ceramic shell with fully or partially electroded circumference. All numerical data were presented for PZT-5 piezoelectric ceramics under "free" and "clamped" mechanical conditions. ECF reaches maximum k = 0.55 for the electrode size of r_0 = 0.85a for central circular electrode arrangement and k = 0.413 for ring electrode covering the radii range $0.6a \le r_0 \le 0.9a$. The maximum ECF calculated for the cylindrical ceramic shell was k = 0.57 for the electrode covering the shell length L_0 = 0.7L (for the shell aspect ratio 2L = 2a, where L and a are the shell's total length and radius). The enhancement of ECF for the partially electroded resonator with respect to the full electrode was also predicted.

The present paper addresses the issues of partially electroded and longitudinally vibrating bar, radially vibrating disc with central circular electrode and radially vibrating ring resonator with partial annular electrode. ECFs are theoretically calculated and experimentally verified by the resonance / antiresonance frequency measurement [3]. This work confirms experimentally previously published theoretical results on the partially electroded disc resonators. ECFs for bar and ring resonators with partial electrodes are theoretically calculated and experimentally measured. The optimum electrode size and the corresponding ECFs were found. The choice of bar and ring resonators with partial electrodes was motivated by the use of such structures in piezoelectric ceramic transformers design – e.g. ring transformer with axisymmetrically divided electrodes or bar transformer with symmetrical or asymmetrical electrode pattern. Ceramic resonators in the shape of ring made from hard PZTs are also typically used for the ultrasound generation in ultrasonic welding and cleaning technology – e.g. in Langevin transducer design. Partially electroded bar and ring resonators were not reported previously, neither theoretically, nor experimentally. One type of soft PZT (APC850) and one type of hard PZT (APC841) was selected for experiments in order not to limit our results only for one specific PZT type.

2. Theoretical considerations

For the calculation of the resonator's electrical impedance/admittance, we adopted one-dimensional vibration modes for thin bar, thin disc and thin ring. Equation of motion:

$$T_{ij,j} = \rho \ddot{u}_i, \quad i = 1,2,3 \tag{2}$$

and Maxwell's equation for non-conducting medium:

$$D_{i,i} = 0, \tag{3}$$

will be solved for the piezoelectric ceramics medium. Piezoelectric equations of state:

$$S_\alpha = s^E_{\alpha\beta} T_\beta + d_{i\alpha} E_i \tag{4}$$

$$D_i = d_{i\alpha} T_\alpha + \varepsilon^T_{ij} E_j \tag{5}$$

are defined by the crystallographic symmetry of ceramics material. The electrode's material and its thickness are not taken into account. The elastic strain tensor is defined by the derivatives of displacement components:

$$S_{ij} = \frac{1}{2}\left(u_{i,j} + u_{j,i}\right) \tag{6}$$

and the electric field by the electric potential derivative:

$$E_i = -\Phi_{,i} \tag{7}$$

The electrical impedance of the resonator is calculated from the displacement current:

$$I = \frac{\partial}{\partial t}\left(\int_{(S)} D_3 dS \right) \tag{8}$$

where the electric displacement is integrated over the electrode surface. The electrical admittance is a ratio of the displacement current and the input voltage:

$$Y = -\frac{I}{Ue^{j\omega t}} \tag{9}$$

2.1. Partially electroded thin bar – transverse longitudinal mode

Mechanical stress/strain system for the thickness-poled and longitudinally vibrating thin bar is given by only one non-zero stress component ($T_1 \neq 0$) and one electrical field/displacement ($E_3 \neq 0$, $D_3 \neq 0$) – for coordinate system see Fig. 1.

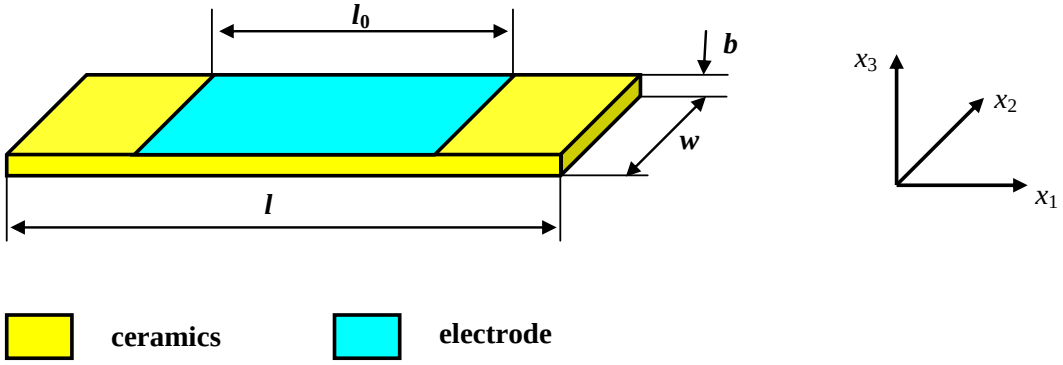

Fig. 1. *Partially electroded bar resonator – thickness poled*

Boundary conditions include mechanically free ends of bar (i.e. $T_1 = 0$) and the continuity of mechanical stress / displacement at the electrode edges. After the calculations described above, we can derive the formula for the electrical admittance:

$$Y = j\omega\left(\varepsilon_{33}^{T}\frac{wl_0}{b}\right)\left\{1-k_{31}^2+k_{31}^2\frac{\sin(\frac{l_0}{l}\eta)\cos((1-\frac{l_0}{l})\eta)}{\frac{l_0}{l}\eta\cos(\eta)}\right\} \tag{10}$$

where

$$\eta = \frac{1}{2}kl, k = 2\pi f\sqrt{\rho s_{11}^E}$$

In a limiting case of the fully electroded resonator (i.e. $l_0 \rightarrow l$), the formula is reduced to the admittance of bar resonator [3].

$$Y = j\omega\left(\varepsilon_{33}^{T}\frac{wl}{b}\right)\left\{1-k_{31}^2+k_{31}^2\frac{\tan(\eta)}{\eta}\right\} \tag{11}$$

The resonance condition for the partially electroded resonator is the same as for the fully electroded one:

$$\eta_r = \frac{\pi}{2}, \frac{3\pi}{2}, \frac{5\pi}{2}, \ldots \tag{12}$$

but the antiresonance condition includes the dimension of the electroded resonator's part in a transcendental equation:

$$1-k_{31}^2+k_{31}^2\frac{\sin(\frac{l_0}{l}\eta_a)\cos((1-\frac{l_0}{l})\eta_a)}{\frac{l_0}{l}\eta_a\cos(\eta_a)} = 0 \tag{13}$$

2.2. Thin bar with embedded electrodes – longitudinal mode

Mechanical stress / strain system for the longitudinally-poled and longitudinally vibrating thin bar is given by only one non-zero stress component ($T_3 \neq 0$) and one electrical field / displacement ($E_3 \neq 0, D_3 \neq 0$) – for coordinate system, see Fig. 2.

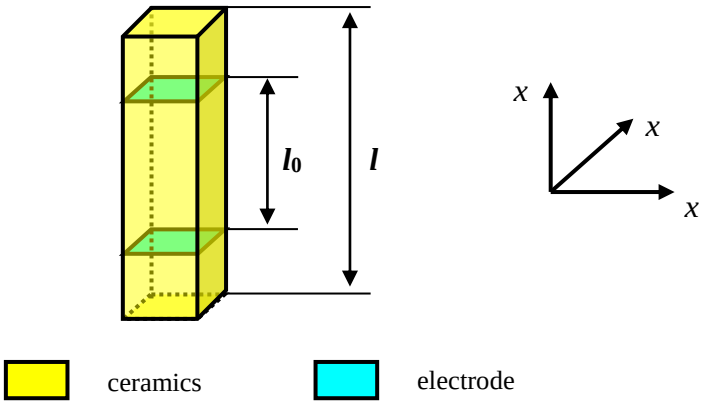

Fig. 2. *Bar resonator with embedded electrodes – longitudinally poled*

Boundary conditions include mechanically free ends of bar (i.e. $T_3 = 0$) and the continuity of mechanical stress / displacement at the electrode edges. After the calculations described above, we can derive the formula for the electrical impedance:

$$Z = \frac{1}{j\omega\left(\varepsilon_{33}^{T}\frac{S}{l_0}\right)\left(1-k_{33}^2\right)}\left\{1-k_{33}^2\frac{\sin(\frac{l_0}{l}\eta)\cos((1-\frac{l_0}{l})\eta)}{\frac{l_0}{l}\eta\cos(\eta)}\right\} \quad (14)$$

where $\eta = \frac{1}{2}kl, k = 2\pi f\sqrt{\rho s_{33}^D}$ and S is the electrode area. In a limiting case of the fully electroded resonator (i.e. $l_0 \to l$), the formula is reduced to the impedance of bar resonator [3].

$$Z = \frac{1}{j\omega\left(\varepsilon_{33}^{T}\frac{S}{l_0}\right)\left(1-k_{33}^2\right)}\left\{1-k_{33}^2\frac{\tan(\eta)}{\eta}\right\} \quad (15)$$

The antiresonance condition is the same as for the fully electroded resonator

$$\eta_a = \frac{\pi}{2}, \frac{3\pi}{2}, \frac{5\pi}{2}, \ldots \quad (16)$$

but the resonance condition depends on the dimension of the electroded part

$$1-k_{33}^2\frac{\sin(\frac{l_0}{l}\eta_r)\cos((1-\frac{l_0}{l})\eta_r)}{\frac{l_0}{l}\eta_r\cos(\eta_r)} = 0 \quad (17)$$

2.3. Partially electroded thin disc – planar mode

Mechanical stress / strain system for the thickness-poled and radially vibrating thin disc is given by non-zero radial and thickness displacement components ($u_r \neq 0, u_z \neq 0$) and one electric field / displacement component ($E_3 \neq 0, D_3 \neq 0$) – for coordinate system, see Fig. 3.

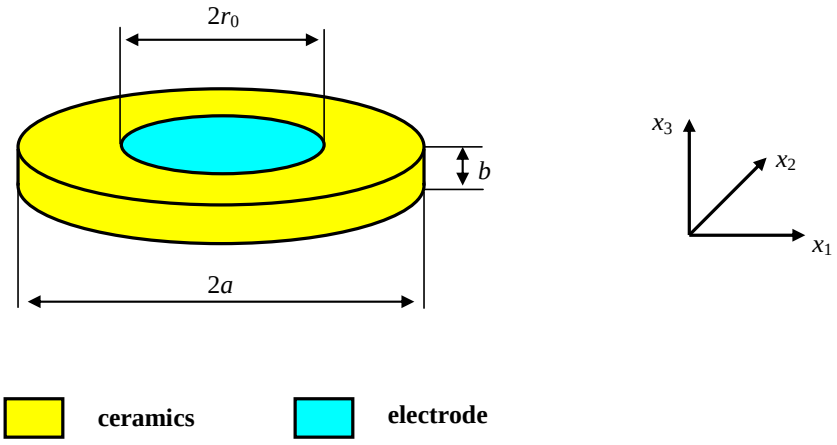

Fig. 3. *Partially electroded disc resonator – thickness poled*

Boundary conditions include mechanically free outer disc circumference (i.e. $T_r = 0$) and the continuity of mechanical stress / displacement at the electrode edges. We use the calculation method published in [8] for homogeneously poled thin ceramic discs. The resonator's admittance could be calculated as:

$$Y = j\omega\left(\varepsilon_{33}^{P}\frac{\pi r_0^2}{b}\right)\left\{1+\frac{k_p^2(1+\sigma^E)}{1-k_p^2}\frac{J_0(\frac{r_0}{a}\eta)}{K_1(\eta)}\frac{K_1(\eta)Y_1(\frac{r_0}{a}\eta)-K_2(\eta)J_1(\frac{r_0}{a}\eta)}{K_1(\frac{r_0}{a}\eta)Y_1(\frac{r_0}{a}\eta)-K_2(\frac{r_0}{a}\eta)J_1(\frac{r_0}{a}\eta)}\right\} \quad (18)$$

where $K_1(\eta) = J_0(\eta)\eta - (1-\sigma^E)J_1(\eta)$;
$K_2(\eta) = Y_0(\eta)\eta - (1-\sigma^E)Y_1(\eta)$;
$\eta = 2\pi f a\sqrt{\rho/c_{11}^P}$; σ^E is Poisson's ratio, $\varepsilon_{33}^P = \varepsilon_{33}^S + \frac{e_{33}^2}{c_{33}^E}$; $c_{11}^P = c_{11}^E - \frac{\left(c_{13}^E\right)^2}{c_{33}^E}$; k_p is planar electromechanical coupling factor and J_0, J_1; Y_0, Y_1 are zero- and first-order Bessel's functions of the first and second kind. In a limiting case of the fully electroded disc (i.e. $r_0 \to a$), admittance is reduced to the known formula for disc resonator [3]:

$$Y = j\omega\left(\varepsilon_{33}^{P}\frac{\pi a^2}{b}\right)\left\{1+\frac{k_p^2(1+\sigma^E)}{1-k_p^2}\frac{J_0(\eta)}{K_1(\eta)}\right\} \quad (19)$$

The resonance condition for the homogeneous disc resonator is identical with the zero value for the denominator in Eq. (18).

$$K_1(\eta_r)\left[K_1(\frac{r_0}{a}\eta_r)Y_1(\frac{r_0}{a}\eta_r)-K_2(\frac{r_0}{a}\eta_r)J_1(\frac{r_0}{a}\eta_r)\right]=0 \quad (20)$$

The antiresonance condition is:

$$1+\frac{k_p^2(1+\sigma^E)}{1-k_p^2}\frac{J_0(\frac{r_0}{a}\eta_a)}{K_1(\eta_a)}\frac{K_1(\eta_a)Y_1(\frac{r_0}{a}\eta_a)-K_2(\eta_a)J_1(\frac{r_0}{a}\eta_a)}{K_1(\frac{r_0}{a}\eta_a)Y_1(\frac{r_0}{a}\eta_a)-K_2(\frac{r_0}{a}\eta_a)J_1(\frac{r_0}{a}\eta_a)}=0 \tag{21}$$

2.4. Partially electroded thin ring – planar mode

A similar calculation method like the one used for thin disc, stress / strain system and boundary conditions (including the free ring's inner diameter circumference) was also adopted for thin partially electroded ring vibrating radially - for geometry, see Fig. 4.

The admittance of such a resonator is ($\eta = 2\pi f a_2\sqrt{\rho/c_{11}^P}$).

$$Y = j\omega\left(\varepsilon_{33}^P\frac{\pi(r_2^2-r_1^2)}{b}\right)\left\{1-\frac{k_p^2(1+\sigma^E)}{1-k_p^2}\times\right.$$

$$\times\left[\frac{K_2(\eta)K_2(\frac{a_1}{a_2}\eta)\left(\frac{r_2}{a_2}\eta J_1(\frac{r_2}{a_2}\eta)-\frac{r_1}{a_2}\eta J_1(\frac{r_1}{a_2}\eta)\right)}{\eta^2(\frac{r_2^2}{a_2^2}-\frac{r_1^2}{a_2^2})\left[K_1(\frac{a_1}{a_2}\eta)K_2(\eta)-K_1(\eta)K_2(\frac{a_1}{a_2}\eta)\right]}-\right.$$

$$\left.-\frac{K_2(\eta)K_1(\frac{a_1}{a_2}\eta)\left(\frac{r_2}{a_2}\eta Y_1(\frac{r_2}{a_2}\eta)-\frac{r_1}{a_2}\eta Y_1(\frac{r_1}{a_2}\eta)\right)}{\eta^2(\frac{r_2^2}{a_2^2}-\frac{r_1^2}{a_2^2})\left[K_1(\frac{a_1}{a_2}\eta)K_2(\eta)-K_1(\eta)K_2(\frac{a_1}{a_2}\eta)\right]}\right]\times$$

$$\times\left[\frac{\eta\frac{r_1}{a_2}\left[K_2(\frac{a_1}{a_2}\eta)J_1(\frac{r_1}{a_2}\eta)-K_1(\frac{a_1}{a_2}\eta)Y_1(\frac{r_1}{a_2}\eta)\right]}{K_2(\frac{a_1}{a_2}\eta)\left[K_1(\frac{r_1}{a_2}\eta)Y_1(\frac{r_1}{a_2}\eta)-K_2(\frac{r_1}{a_2}\eta)J_1(\frac{r_1}{a_2}\eta)\right]}+\right.$$

$$\left.+\frac{\eta\frac{r_2}{a_2}\left[K_1(\eta)Y_1(\frac{r_2}{a_2}\eta)-K_2(\eta)J_1(\frac{r_2}{a_2}\eta)\right]}{K_2(\eta)\left[K_1(\frac{r_2}{a_2}\eta)Y_1(\frac{r_2}{a_2}\eta)-K_2(\frac{r_2}{a_2}\eta)J_1(\frac{r_2}{a_2}\eta)\right]}\right]-$$

$$\left.-\frac{k_p^2(1+\sigma^E)}{1-k_p^2}\frac{\eta\frac{r_1}{a_2}\left(\frac{r_2}{a_2}\eta Y_1(\frac{r_2}{a_2}\eta)-\frac{r_1}{a_2}\eta Y_1(\frac{r_1}{a_2}\eta)\right)\left[J_1(\frac{r_1}{a_2}\eta)K_2(\frac{a_1}{a_2}\eta)-Y_1(\frac{r_1}{a_2}\eta)K_1(\frac{a_1}{a_2}\eta)\right]}{K_2(\frac{a_1}{a_2}\eta)\left[K_1(\frac{r_1}{a_2}\eta)Y_1(\frac{r_1}{a_2}\eta)-K_2(\frac{r_1}{a_2}\eta)J_1(\frac{r_1}{a_2}\eta)\right]}\right. \tag{22}$$

Resonance and antiresonance follow the same conditions ($Y\to\infty$ for resonance and $Y\to 0$ for antiresonance), but the formulae are not listed here because of their long expressions.

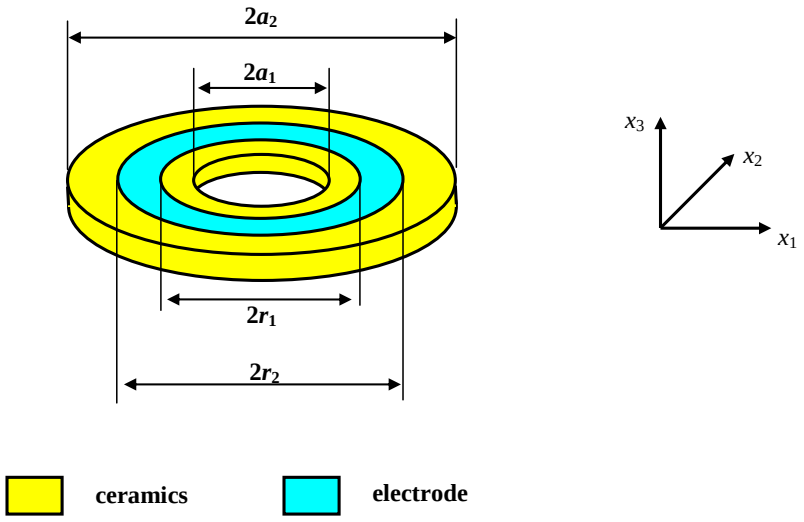

Fig. 4. *Partially electroded ring resonator – thickness poled*

3. Experiment and numerical calculations

Resonance and antiresonance wave numbers η_r and η_a were calculated as solutions of Eqs. (12) and (13) for a thin bar in transverse longitudinal vibration mode, Eqs. (16) and (17) for a thin bar in longitudinal mode, Eqs. (20) and (21) for a thin disc vibrating in radial mode and from Eq. (22) for a thin ring. Resonance and antiresonance frequencies are simply related to the wave numbers for each vibration mode. Therefore ECF's definition - Eq. (1) - could be written as:

$$k_{eff}^2 = \frac{\eta_a^2 - \eta_r^2}{\eta_a^2} \tag{23}$$

For the numerical values of material property coefficients used in calculations, see Table 1.

Table 1. *Material properties of PZT ceramics used in calculations*

Ceramics type	k_{31} [-]	k_{33} [-]	k_p [-]	σ^E [-]
APC841 Hard PZT	0.27	0.63	0.60	0.30
APC850 Soft PZT	-	-	0.63	0.35

Partially electroded resonators were accomplished for bar, disc and ring resonators from soft and hard PZT ceramics (APC International Ltd., Mackeyville, PA, USA). Electrodes were deposited by air-dry Ag-paste (Agar Scientific, Silver paint type G302). Impedance spectra were measured by Agilent 4294A Impedance analyzer.

Samples of partially electroded disc resonators were prepared from soft PZT ceramics, type APC850. Disc dimensions were 20 mm diameter and 1.78 mm thickness and 26.25 mm diameter and 2 mm thickness. A set of samples with electrode aspect ratios ranging from 0.1 to 1.0 was prepared for both dimensions. Samples of partially electroded bar resonators were made from hard PZT, type APC841. Sample dimensions were 49.6 mm long, 6 mm wide and 0.5 mm thick. A set of samples with electrode aspect ratios from 0.1 to 1.0 was prepared. The samples of partially electroded ring resonators were made from hard PZT, type APC841. The ring inner diameter was 20 mm, outer diameter 50 mm and thickness 6 mm. Because there are too many combinations of dimensions, only three sets of samples were prepared. The first set was from samples with outer electrode diameter equal to the ring outer diameter. The second set of samples included samples with electrode inner diameter equal to the ring inner diameter. The samples in the third set had electrodes distributed symmetrically with respect to the center diameter (35 mm diameter) – for details on dimensions, see Table 2.

Table 2. *Dimensions of partially electroded ring resonators (total diameter 20 mm/50 mm/thickness 6 mm)*

Set No.	Inner electrode diameter/outer electrode diameter [mm]				
1	24/50	28/50	32/50	36/50	40/50
2	20/30	20/34	20/38	20/42	20/46
3	32/38	29/41	26/44	23/47	-

4. Results and discussion

ECF for partially electroded bar resonators (k_{31}-mode) shows dependence on the electroded part aspect ratio (i.e. l_0/l) with saturated value starting at the aspect ratio l_0/l = 0.6 – see Fig. 5. Calculated data fits experimental data for all aspect ratios. Maximum ECF k_{eff} = 0.26 was measured for the electrode size aspect ratio equal to l_0/l = 0.75 for k_{31}-mode for the bar resonator.

Calculations for the bar resonator vibrating in k_{33}-mode (Fig. 6) show similar aspect ratio dependence as the bar resonator working in k_{31}-mode, but with higher values of ECF due to the higher electromechanical coupling factor k_{33} of used PZT. Maximum ECF k_{eff} = 0.67 was calculated for the electrode size aspect ratio equal to l_0/l = 0.75 for k_{33}-mode for the bar resonator with embedded electrodes.

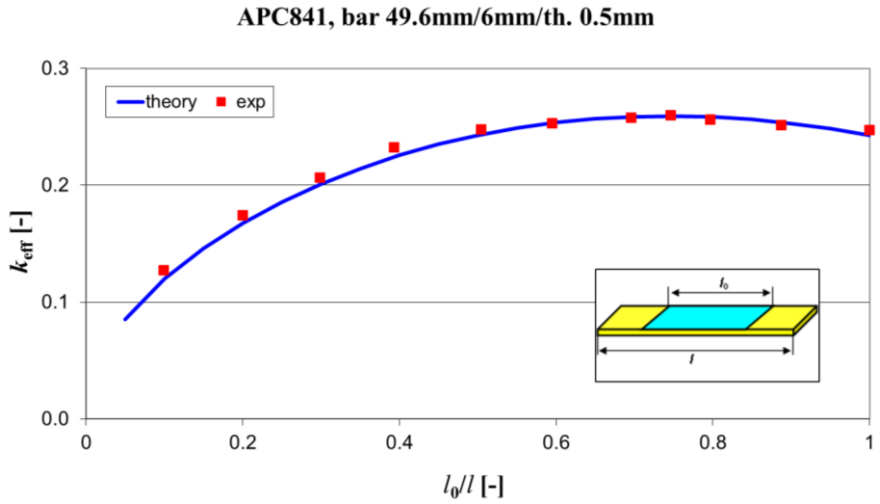

Fig. 5. *Effective coupling factor for partially electroded bar resonators (k_{31}-mode, APC841, 49.6 mm x 6 mm x 0.5 mm)*

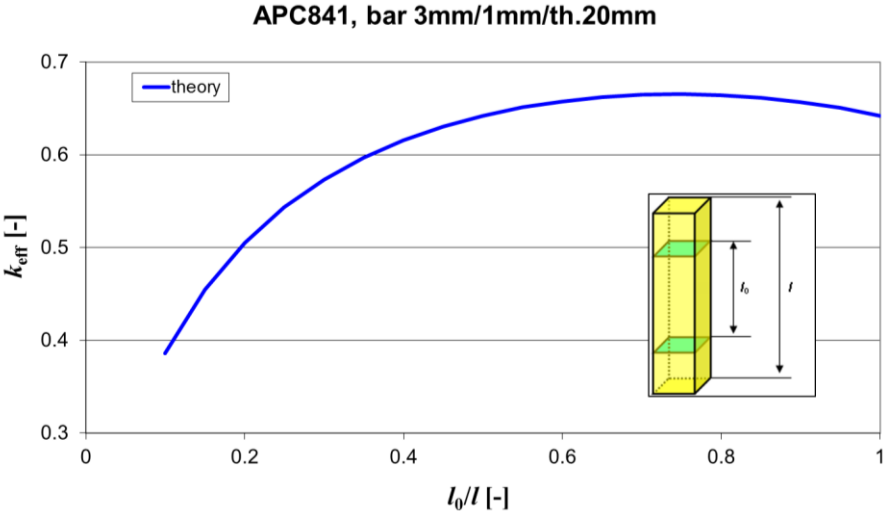

Fig. 6. *Effective coupling factor for the bar resonators with embedded electrodes (k_{33}-mode, APC841, 20 mm x 3 mm x 1 mm)*

ECFs for partially electroded disc resonators (k_p-mode) show saturation at the aspect ratio (i.e. electrode's diameter / total diameter) equal to about r_0/a = 0.7 – see Fig. 7. Calculated data fit the experimental values only for the aspect ratios below r_0/a = 0.5. The approximation employed in calculations is not valid for higher values of aspect ratios, because no electroded outer ring segment can any longer be approximated by the shape of the thin ring. The samples with different disc diameters

exhibit the same behavior in ECF as it is seen in Eq. (18) and in Fig. 7. ECF depends on the values of the electromechanical coupling factor k_p, Poisson's ratio σ^E, but not on the disc diameter like the resonance and antiresonance frequencies themselves. Maximum ECF k_{eff} = 0.58 was measured for the electrode size aspect ratio equal to r_0/a = 0.80 for k_p-mode for the disc resonator. This value agrees well with the previously published [7] theoretical value k_{eff} = 0.55 for the electrode size aspect ratio equal to r_0/a = 0.83 calculated for a different PZT type.

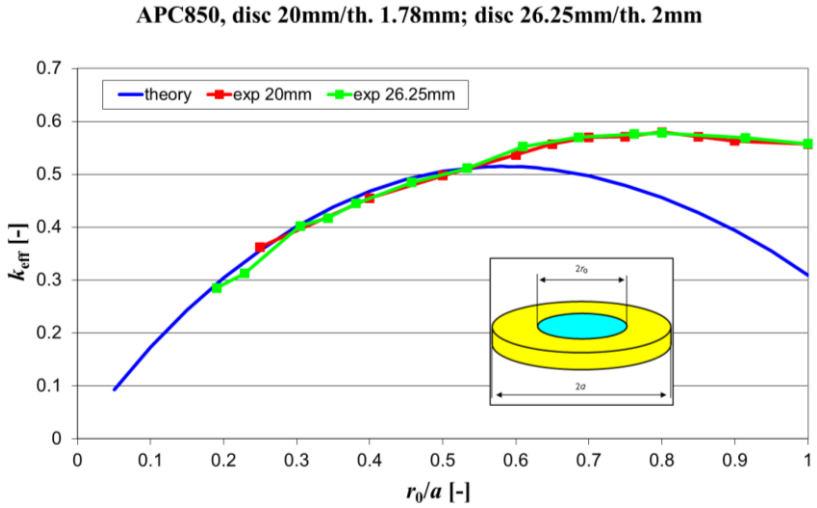

Fig. 7. *Effective coupling factor for partially electroded disc resonators (k_p-mode, APC850, 20 mm diameter / 1.78 mm and 26.25 mm thick / 2 mm thick)*

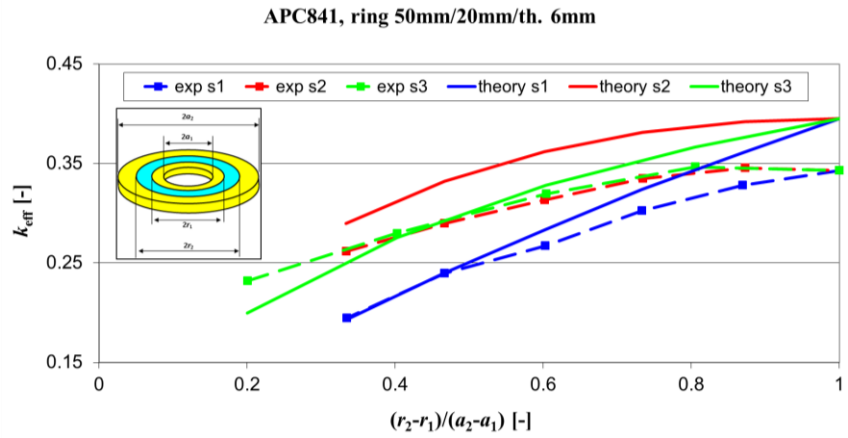

Fig. 8. *Effective coupling factor for partially electroded ring resonators (k_p-mode, APC841, 20 mm/50 mm diameter / 6 mm thickness) as a function of ring electrode relative width*

All three sets of partially electroded rings exhibit the same trend in ECF with the highest value k_{eff} = 0.34 for the ring resonator with full electrode, see Fig. 8. Set No. 1 and 3 fit theoretical calculations up to the electrode width aspect ratio equal to 0.7. Calculations for set No. 2 (inner electrode diameter is equal to disc inner diameter) show higher values than it was measured, on the contrary. Some differences in the calculated values are due to the approximations employed for one-dimensional calculations of ring electrode. Data shows the same trend in the calculated as well as in the measured values of ECF.

5. Conclusions

Effective ECF reaches its top value at an optimum electrode size for all studied resonator cases (bar, disc and ring). Values of effective ECFs were predicted in analytical one-dimensional models for thin bar (k_{31}-mode), thin disc (k_p-mode) and thin ring (k_p-mode) with partial electrodes and thin bar with embedded electrodes (k_{33}-mode). Numerically calculated effective ECFs were measured on the samples of bar, disc and ring resonators with partial electrodes. Maximum effective ECFs were measured:

- k_{eff} = 0.26 for thin bar (k_{31}-mode) for the aspect ratio l_0/l = 0.75
- k_{eff} = 0.58 for thin disc (k_p-mode) for the aspect ratio r_0/a = 0.80
- k_{eff} = 0.34 for thin ring (k_p-mode) for the resonator with full electrode (outer / inner ring diameters are 50 mm/20 mm).

Maximum ECF for bar resonator with embedded electrodes (k_{33}-mode) was calculated as k_{eff} = 0.67 for the electrode aspect ratio l_0/l = 0.75. ECF saturates at the aspect ratio of r_0/a = 0.7 for the thin disc with partial electrode. Ring resonators show the same trend as discs without saturation of ECF. The presented results may serve as a guide for the optimum electrode pattern design for resonators with partial electrodes.

Acknowledgements

This work was supported by ESF operational program "Education for competitiveness" in the Czech Republic within the framework of project "Support of engineering of excellent research and development teams at the Technical University of Liberec" No. CZ.1.07/2.3.00/30.0065.

References

[1]. Chang S. H., Rogacheva N. N., Chou C. C., *Analysis of methods for determining of electromechanical coupling coefficients of piezoelectric elements*, IEEE Transactions on Ultrasonics Ferroelectrics and Frequency Control, 42(4), p. 630-640, 1995.

[2]. Mezheritskiy A. V., *Invariants of electromechanical coupling coefficients in piezoceramics*, IEEE Transactions on Ultrasonics Ferroelectrics and Frequency Control, 50(12), p. 1742-1751, 2003.

[3]. IRE Standards on Piezoelectric Crystals, *Measurement of Piezoelectric Ceramics*, Proceedings of the IRE, 49(7), p. 1161-1169, 1961.

[4]. Huang C. H., Lin Y. C., Ma C. C., *Theoretical Analysis and Experimental Measurement for Resonant Vibration of Piezoceramic Circular Plates*, IEEE Transactions on Ultrasonics Ferroelectrics and Frequency Control, 51(1), p. 12-24, 2004.

[5]. Huang C. H., *Theoretical and experimental vibration analysis for a piezoceramic disk partially covered with electrodes*, The Journal of the Acoustical Society of America, 118(2), p. 751-761, 2005.

[6]. Ivina N. F., *Analysis of the Natural Vibrations of Circular Piezoceramic Plates with Partial Electrodes*, Acoustical Physics 47(6), p. 714-720, 2001.

[7]. Rogacheva N. N., *The dependence of the electromechanical coupling coefficient of piezoelectric elements on the position and size of the electrodes*, Journal of Applield Mathematics and Mechanics, 65(2) p. 317-326, 2001.

[8]. Meitzler A. H., O'Bryan Jr. H. M., Tiersten H. F., *Definition and measurement of radial mode coupling factors in piezoelectric ceramic materials with large variations in Poisson's ratio*, IEEE Transactions on Sonics and Ultrasonics, SU-20(3), p. 233-239, 1973.